Magnetotelluric and magnetovariational measurements in Southwest Bohemia, data presentation and modelling experiments

Václav Červ, Josef Pek and Oldřich Praus

Geophys. Inst., Acad. Sci. Czech Rep., Prague, Czech Republic

Abstract

During the last three years a project of long period geoelectrical studies in Southwest Bohemia, immediately along the German/Czech border, near to the KTB (Oberpfalz, Germany) site, has been solved. A description of the main features of the long period magnetovariational and magnetotelluric data (period range from 10 s to about one hour) from this region is given here. The data seem to roughly fit a model of a 2-D regional structure, striking E-W, overlaid by a highly distorting near-surface layer with solely static effect on the magnetotelluric curves. The distorting layer displays strong anisotropy with preferred conductivity in NW-SE to NNW-SSE direction. Attempt is made to estimate the absolute static shifts of magnetotelluric curves. Several variants of 2-D models for the deep, regional structure are discussed. To discuss possible sources of local distortions, a speculative model with strong anisotropy is presented, which can qualitatively explain the discrepancy of principal directions derived from magnetotelluric impedances, on the one hand, and from induction vectors on the other, within the scope of 2-D structures.

1 Magnetotelluric and magnetovariational experiments

Anomalous geoelectrical effects observed in the immediate neighbourhood of the ultradeep drilling site KTB in the Oberpfalz (Germany) (e.g. [1]) were a strong motive for extending the deep geoelectrical research into a broader vicinity of this locality. The project of deep magnetotelluric (MT) and magnetovariational (MV) soundings in SW Bohemia, in a region which, from the Bohemian side of the German-Czech border, abuts on the KTB locality, was a part of this research programme. Within this project the following field experiments were carried out during the period 1990–1993 (Fig. 1): (i) simultaneous long-period MV measurements (period range from 900 s to about several hours) across an array of 10 field stations covering an area of about 50×50 km^2 between the places Rozvadov–Stříbro–Toužim–Cheb, (ii) long-period MT and MV measurements (period range from 10 s to about one hour) at 14 field stations arranged along a profile, about 100 km in length, between the places Cheb–Rozvadov–Nýrsko; at seven of these stations the audiomagnetotelluric (AMT) data with periods ranging from 10^{-3} to about 10 s were supplemented (in cooperation with the staff and using the AMT/MT equipment of the University of Frankfurt/Main) to infer information on the influence of the shallower conductivity distribution on the MT data, and (iii) AMT measurements, in cooperation with Italian colleagues from the University of Padova and IIRG Pisa, along two local profiles, the first situated near to Tachov, in the northern part of our profile, and the other, in the southern part, near to Kdyně. In this paper attention will be payed to the long-period MT and MV data only, as much of the AMT material is still under processing and under study.

From the geological point of view, the broader FRG/Czech surroundings of the KTB site can be characterized as a region where different zones of the Bohemian Massif, representing the easternmost part of the European Hercynides, make contact [2]. Specifically, the KTB drilling sites, both the pilot and the superdeep, are located near the western margin of the Bohemian Massif, and a few kilometers south of the structurally important boundary of the Moldanubian and Saxothuringian zones of the Central European orogenic belt. The boundary, along which the two segments of the earth crust collided about 320 million years ago and the Moldanubian rocks were overthrusted on the Saxothuringian ones, is believed to be the Erbendorf line. Its continuation into western Bohemia is assumed to be the Litoměřice fault zone,

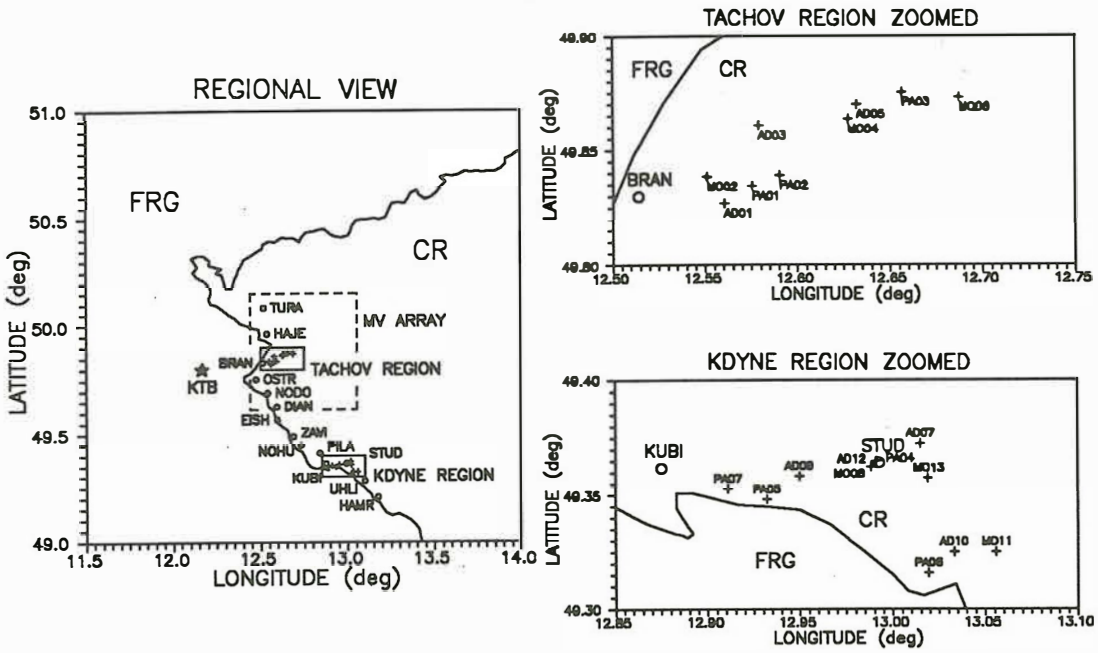

Figure 1: Region of deep geoelectrical experiments in SW Bohemia. Dashed rectangle demarcates a border of the MV array, circles are for long-period MT stations, and within the two boxes, enlarged on the right, two local AMT profiles are shown, measured by Italian colleagues.

situated in the N of our interest region. In the W, this region makes an immediate contact with the KTB area, and on the Czech territory it is demarcated by the Central Bohemian deep fault in the S and the West Bohemian fault zone in the E. The MT profile crosses several geological units belonging both to the Saxothuringian and Moldanubian tectonic units.

2 Magnetovariational transfer functions

A preliminary estimation of the induction effect of the structure involved was based on the analysis of long-period MV data. MV measurements within the array Rozvadov–Toužim–Stříbro–Cheb have already been analyzed in [3] in detail. The main conclusions based on the behaviour both of the single station and reference station geomagnetic transfer functions (with Budkov observatory in South Bohemia as the common reference station) are as follows:

(i) Single station induction vectors, defined in frequency domain as vectors

$$\text{Real } TF = \Big(\Re(W_N), \Re(W_E)\Big), \quad \text{Imag } TF = \Big(\Im(W_N), \Im(W_E)\Big),$$

where $H_Z = W_N H_N + W_E H_E$, H_N, H_E, and H_Z being the north, east, and vertical magnetic component respectively, fit the general over-regional pattern with the predominant orientation towards the S and decreasing moduli towards the E or SE. Single station induction characteristics express rather regional structural features characterized by a predominant E-W strike.

(ii) Reference station vectors, defined in frequency domain as vectors

$$\text{Real } TFR = \Big(\Re(W_N^{REF}), \Re(W_E^{REF})\Big), \quad \text{Imag } TFR = \Big(\Im(W_N^{REF}), \Im(W_E^{REF})\Big),$$

where $H_Z - H_Z^{REF} = W_N^{REF} H_N^{REF} + W_E^{REF} H_E^{REF}$, H_N^{REF} and H_E^{REF} being for the field components at the reference station, exhibit generally decreased moduli at all stations compared with those of single station vectors. Their azimuths are systematically rotated by 30 to 40 degrees towards the SE compared

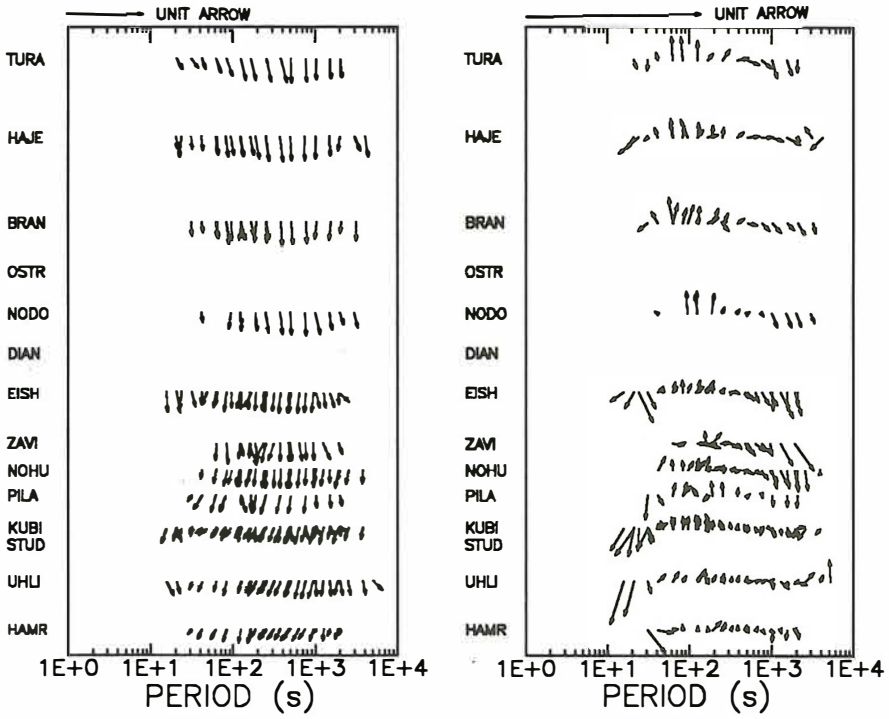

Figure 2: Real and imaginary (left and right, respectively) single station induction vectors along the MT profile Cheb–Tachov–Nýrsko in SW Bohemia within the period range 10–3000 *s*.

to the single station vector orientation. Reference station induction characteristics are formed by local geological features. Their dominating strike is SW-NE which conforms with the main tectonic features of the region (contact zone of the Saxothuringicum and the Moldanubicum, identified with the Erbendorf-Litoměřice fault zone striking SW-NE-ward).

From the MT data collected along the line Cheb–Tachov–Nýrsko only single station transfer functions were evaluated (Fig. 2). Real transfer functions are generally rather large, with the moduli as much as 0.3 in the N of the profile, and directed almost uniformly towards the S. Approaching the southern section of the profile, notably starting from station NOHU, a deflection of the induction vectors by more than 20 degrees towards the W seems to take place. This deflection is first noticable at shorter periods already at stations in the N, from station NOHU towards the S it occurs for longer periods as well. Induction response measured by the moduli of the real induction vectors seems to decrease progressively from the N to the S.

Imaginary transfer functions (Fig. 2) are very small compared with the real ones. Consequently, a large scatter of azimuths is their characteristic feature. In an apparently chaotic distribution of the imaginary vectors, certain regularity seems to persist anyway, consisting in the existence of a zone of antiparallel orientation, in relation to the real vectors, within the range of periods of about a few tens of seconds to approximately 1000 *s*.

3 Magnetotelluric data and magnetotelluric parameters

MT data are in general more informative, especially as regards the vertical resolution of the conductivity distribution, but they are highly sensitive to various distortions, caused by the industrial, man-made noise, affecting raw time series, as well as by 'geological noise'.

MT data along our profile generally display rather 3-D character, which can be evidenced by 'crest representations' of the impedances at individual stations for a few periods shown in Fig. 3.

From this figure, we can draw some more information concerning two basic classical MT parameters - Swift's principal direction and anisotropy.

For any of the stations Swift's principal direction is stable, within a few degrees, throughout the whole

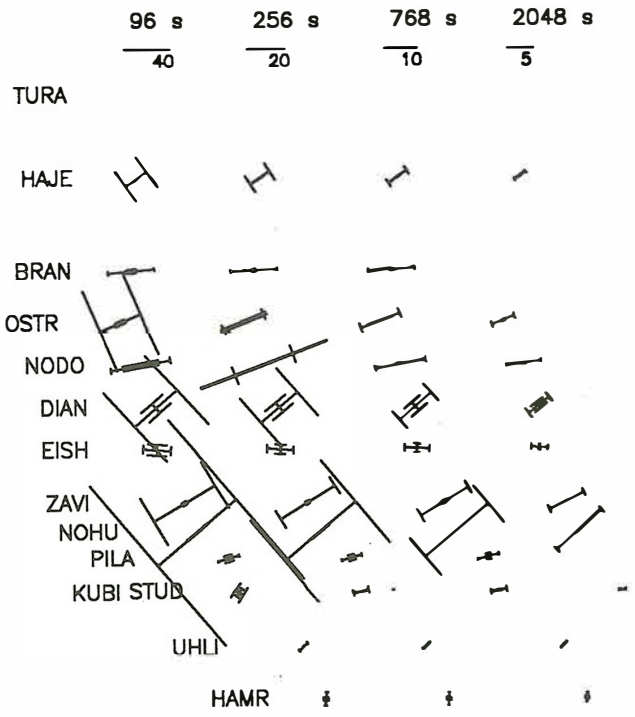

Figure 3: 'Crest representations' of MT impedances along the MT profile for a representative set of periods. The crests are oriented into respective Swift's principal directions and express the main impedances. Perpendicularly to them, the corresponding diagonal impedances are plotted.

period range from 10 to about 1000 s. It varies, however, non-systematically from station to station, although the major axes of the polar impedance diagrams are mostly found within the octant from 45 to 90 degrees.

Anisotropy of the MT curves, defined by the ratio max/min impedance in the polar diagram, is another characteristics stable with period, but variable from station to station. MT anisotropy is generally large at most of the stations involved, typically around 10, reaching its maximum near to station NOHU (as much as 10^2).

Another classical MT parameter, skew, defined by ratio $\frac{|Z_{xx}+Z_{yy}|}{|Z_{xy}-Z_{yx}|}$, varies rather randomly along the profile. In Fig. 4 skew is shown as a 3-D plot along the profile and compared with the error parameter $\frac{\sqrt{\delta Z_{xy}^2+\delta Z_{yx}^2}}{|Z_{xy}-Z_{yx}|}$, [4]. From this figure we can see that, at most of the stations, the skew is too large to allow a 1-D local approximation of the structure to be accepted. It reaches its minimum at station BRAN, which seems to be the only station where the condition of zero skew, and consequently of minimum (or

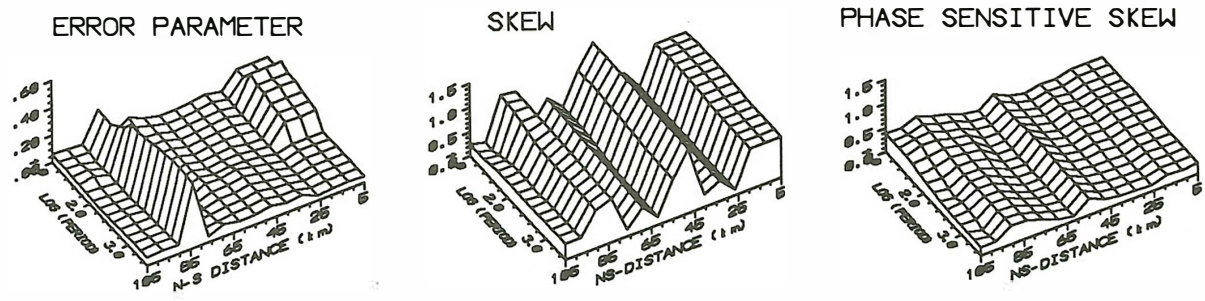

Figure 4: Error parameter, classical skew, and phase sensitive skew along the profile for the whole period range covered. For the position along the profile, see Fig. 8.

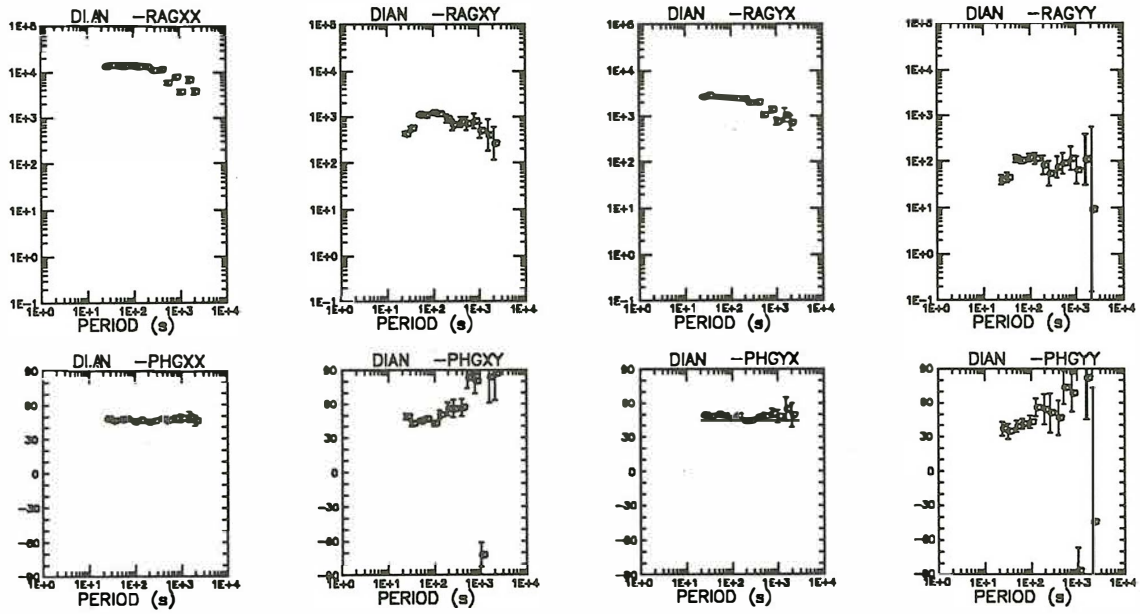

Figure 5: Complete set of apparent resistivities and phases at station DIAN, in geographical coordinates.

apparent minimum) effect of 3-D distortions can be reasonably accepted.

To summarize, the principal features of MT data seem to contradict the simple conclusion on the E-W strike of the structure, derived earlier from the induction arrows. MT polar impedance diagrams would rather indicate SE-NW or SSE-NNW as a direction of preferred conductivity within the structure. This pattern is characteristic not only for the data from SW Bohemia, but seems to be of more regional extent, as indicated in [5] and [6] by MT data from the Oberpfalz (Germany). In principle, three possible sources of this discrepancy, or more likely a combined effect of all of them, may be considered—an entirely 3-D character of the structure, galvanic distortions of the MT data, and physical macro-anisotropy of the electric conductivity within the structure on the regional scale.

4 Distortions of magnetotelluric data

The idea of rather strong galvanic distortions of the MT data along the whole profile seems to be supported by rather random fluctuations of all the classical MT parameters over distances of a few kilometers only, which certainly does not indicate that the deep structure varies so dramatically across such short distances. Taking the typically high resistivities in the area, often more than 10^3 Ωm, into account, we must emphasize, however, that the 'near-surface' character of the distorting structures may in fact represent a distorting layer several kilometers thick here, if periods greater than 10 s are considered.

Visual inspection of MT curves can give a qualitative idea as to the character of the distortions. For the major part of the profile, particularly northernward of station KUBI, the sounding curves show similar features, illustrated here for station DIAN in geographical coordinates (Fig. 5). One pair of impedance components, specifically Z_{xx} and Z_{yx}, dominates the impedance tensor. Phases within the individual columns of the impedance tensor are close to each other, at least for longer periods above 100 s. The latter feature is almost perfectly expressed for the dominating impedance pair, whereas it is less convincing, and, due to greater errors, partly hidden for the other pair of impedances, i.e. Z_{xy} and Z_{yy}. Physically these impedance relations suggest a dominant role of the H_x, i.e. northern component of the geomagnetic variation field in the induction process. The electrical field is thus controlled mainly by a single magnetic component, and the telluric components E_x and E_y are highly correlated. In terms of static distortions, the above impedance relations would indicate a 2-D regional structure, striking nearly E-W or N-S , and an additional galvanic distortion described by a static tensor with one dominating column, resulting physically in a pronounced linear polarization of the telluric field.

Additional support to the hypothesis of strong static distortions of the MT data is given by inspecting the phase sensitive skew [4] along the profile and for the period range covered (Fig. 4). Except the

anomalous zone near the southern end of the profile, this parameter is mostly less than 0.3, indicating thus that a substantial part of the 3-D effects originates in near-surface inhomogeneities.

Attempts to verify the above scheme quantitativelly and to carry out exact separation of the local and regional contributions to the impedances were successful only partially, specifically with MT data from station OSTR [7]. Introducing Bahr's δ-model [8], we succeeded in identifying a regional strike close to the geographical directions and a local (apparent) strike closely related to the azimuths of the reference station real induction arrows. Additionally, we attempted to estimate the absolute static shifts by repeating Eisel's approach [5], i.e. to fit the long period branches of MT curves at a chosen MT station to Schmucker's continental MT curve through deshifted data of an intermediate nearby station Hanfmühl (Germany). Though this approach may seem rather crude with our data, we obtained an estimate of the static shifts characterized by a telluric ellipse oriented approximately in the direction of the apparent local strike. After deshifting the data from OSTR, the anisotropy of the regional impedance almost disappeared.

At other stations along the profile the exact distortion analysis was less successful for large instabilities of the decomposition parameters.

5 Station OSTR as a reference for distortion estimates

MT data from station OSTR (Ostrůvek) were already extensively analyzed in [7], and, as mentioned above, a rough estimate of the absolute MT distortion parameters was tried for this station. In what follows an attempt is made to use those results for estimating the degree of galvanic distortions at the other stations along the profile, where a direct decomposition was much less successful. For this purpose a two-step-procedure is used. First, the inter-station MT transfer functions with respect to OSTR, $\mathbf{A}_{\mathrm{STAT,OSTR}}$, are evaluated, defined as $\mathbf{Z}_{\mathrm{STAT}} = \mathbf{A}_{\mathrm{STAT,OSTR}}\,\mathbf{Z}_{\mathrm{OSTR}}$, where $\mathbf{Z}$ is the impedance tensor. The point is that if the inter-station MT transfer function $\mathbf{A}_{\mathrm{STAT,OSTR}}$ is real and frequency independent then the same deep, regional structure may be assumed below both STAT and OSTR. These two localities then can be considered as differring in the near-surface electrical conditions only, which generate different galvanic distortions. In such a way a structural continuity of the regional structure can be traced. In second step, the inter-station MT transfer functions are multiplied by the absolute distortion matrix of OSTR, $\mathbf{A}_{\mathrm{STAT}} = \mathbf{A}_{\mathrm{STAT,OSTR}}\,\mathbf{A}_{\mathrm{OSTR}}$, yielding thus the absolute distortion matrix for the current station STAT.

Before showing any results, it must be emphasized that all the estimates presented below are of essentially qualitative character, as some highly approximate steps are involved in applying the procedure. Particularly the following ones should be explicitely mentioned:

(i) Already the decomposition of the MT tensor at OSTR, presented in [7], was carried out by a rather simplified approach of Eisel [5]—the long period branches of the 'deskewed' curves from OSTR were fitted to the univariate main impedances from the intermediate station HAM (Hanfmühl, Germany), which had been pre-processed by their 'deshifting' with respect to Schmucker's continental deep sounding curve.

(ii) With our data, the inter-station MT transfer functions can be considered constant and real for very long periods only, typically starting from a few hundreds of seconds towards longer periods. For these periods, however, the error bars for these functions are usually quite large, often exceeding the respective mean values, so that the statistical uncertainty of the resulting estimates is very high.

(iii) Since the variability of the inter-station MT transfer functions for the deep, regional structure alone is often quite weak (e.g. not more than 20 per cent for model B1 in Fig. 8), experimental data of extremely good quality are required to identify changes of the regional conductivity distribution in the inter-station MT transfer functions.

In Fig. 6a the inter-station MT transfer functions are presented in a form of telluric ellipses, expressing how a circularly polarized telluric field at station OSTR would be distorted at other stations if the impedance differences between the individual stations were caused solely by galvanic distortions.

Taking the rough estimate of the absolute distortion matrix for station OSTR [7], which makes $\mathbf{A}_{\mathrm{OSTR}} \approx \begin{pmatrix} 1.2 & 4.5 \\ 0.6 & 6.5 \end{pmatrix}$ for periods greater than about 100 s, the relative inter-station MT transfer functions can be multiplied by this matrix to give estimates of absolute distortion matrices at other stations as well. After doing so, the corresponding absolute telluric ellipses can be drawn at selected stations along the profile (Fig. 6). They express how a normalized, circularly polarized telluric field at infinity would be distorted by the local galvanic distortions at individual stations.

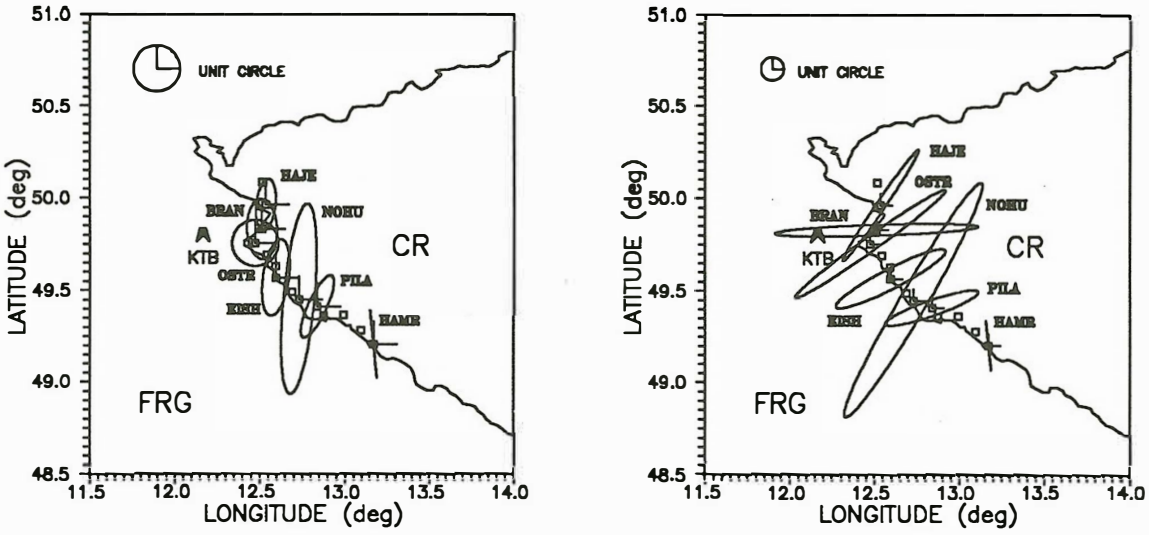

Figure 6: Relative telluric ellipses with respect to OSTR (a), and estimates of absolute distortion ellipses (b) at individual MT stations along the profile.

Similarly as at OSTR, the absolute telluric ellipses at other stations indicate extreem distortions of the telluric field throughout the region involved. A common characteristic feature is large eccentricity of the telluric ellipses, indicating large conductance anisotropy (either apparent or real) of subsurface structures. The direction of preferred conductivity of the distorting structures, indicated by minor axes of telluric ellipses, is SE-NW to SSE-NNW at most of the stations.

Rather exceptional features exhibits station BRAN with its telluric ellipse oriented almost perfectly into geographical axes. Although seemingly the least 3-D distorted station, it seems to exhibit large shifts in geographical directions, particularly E-W, which incidentally coincides with the assumed regional strike. This shift explains the extreme anisotropy of MT curves at BRAN as an effect of static amplification of the yx-resistivity curve by nearly two orders of magnitude, leaving the small skew almost unaffected. This effect may be also responsible for only little success in using BRAN as a reference in estimating inter-station MT transfer functions in [9], where no acceptable period-independence of the inter-station distortion parameters could be achieved with BRAN as a common reference, apparently due to amplification of fluctuations in MT data via the large distortion parameters of the reference station.

Another station obviously distorted by an additional local distortion effect is NOHU with the largest telluric ellipse. At station HAMR, at the southern end of the profile, the telluric parameters become physically unacceptable ($a_{yy} < 0$), which indicates that more substantial changes of the deeper, regional conductivity structure are likely to take place when approaching the southern section of the profile.

6 Formal 1-D modelling of roughly 'deshifted' MT data

To get a rough idea about resistivities beneath the profile, 1-D inversion of the MT curves, 'deshifted' by the distortion parameters estimated above, was carried out, separately for each station's E (i.e. E-W) and H (i.e. N-S) curves. For the inversion, the controlled random search procedure [10] was used which allows noisy experimental data to be mapped onto a whole set of acceptable structural models. Both resistivity and phase curves were inverted simultaneously, and a slightly greater weight was put on phases. As the curves were constructed under the assumption of a common regional structure, verified roughly for stations along the northern and central part of the profile, as far as PILA, the inversion should provide us with roughly identical models at individual stations, representing a generalized model of the regional basement.

Inversion of E-curves (Fig. 7) shows, except the very superficial layers which are purely reflected by the data available, a rather homogeneous conductivity structure beneath the whole profile, with slightly decreasing conductivity towards the S. A relatively thin resistive inter-layer, found in almost all models,

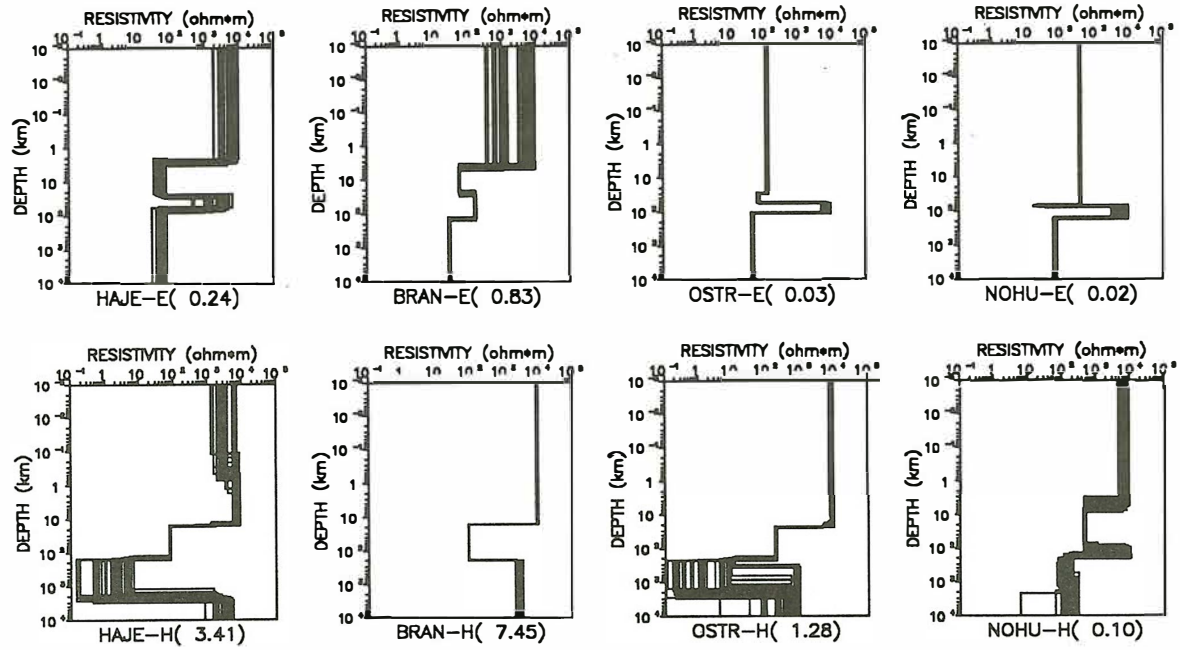

Figure 7: 1-D formal inversion of 'deshifted' MT curves at selected stations along the profile. Top row of plots—inversion of E-curves, bottom row—inversion of H-curves.

seems to be significant for fitting the phases properly.

H-curves give more complex sections, with typically two levels of conductivity increase—the first at depths of about $10 - 20$ km, and the other at $100 - 200$ km, except site BRAN where only the shallower conductivity jump is indicated.

Inspecting both sets of 1-D inversion results, the H-curves give systematically a more resistive structure near the surface and a more conductive deep basement as compared to E-curves. Although the most substantial part of the anisotropy of MT curves disappered after we had tried to roughly eliminate the galvanic distortions, a systematic difference between the two MT field modes persists in the data along the whole northern and central part of the profile, indicating an authentically 2-D character of the regional structure within the area under study.

7 2-D modelling experiments

Most of the modelling experiments presented below are based on the assumption that the structure may be decomposed into a 2-D regional substratum, striking E-W, and a generally 3-D near-surface distorting layer with only static effect on MT data within the period range considered, i.e. for periods greater than about 10 s. A lot of material presented in the preceding sections aimed at founding this hypothesis. Considering such a structural outline, we assume that the observed induction arrows, as well as phases of both MT impedances, Z_{yx} for E-polarization and Z_{xy} for H-polarization, in geographical coordinates, are undistorted functions of the regional structure and can be used immediately to model the regional conductivity distribution.

First 2-D modelling experiments aimed at proposing minimum structures which would explain the induction arrows alone. It was a rather problematic task, as no outstanding features, such as azimuth inversions, are observed in the induction arrows along the profile. Generally low resolution of MV data allows the moduli of induction vectors to be explained by a whole family of various models. They have, however, one common feature—they all require a good conductor further to the N of our profile. The conductivity contrast on this contact seems to be the primary source of relatively large induction vectors. The nature of the contact, its distance and vertical extent may range within broad limits, and are not unambiguosly reflected by the available data.

Particular interpetation attempts were based on several different initial structural hypotheses and on

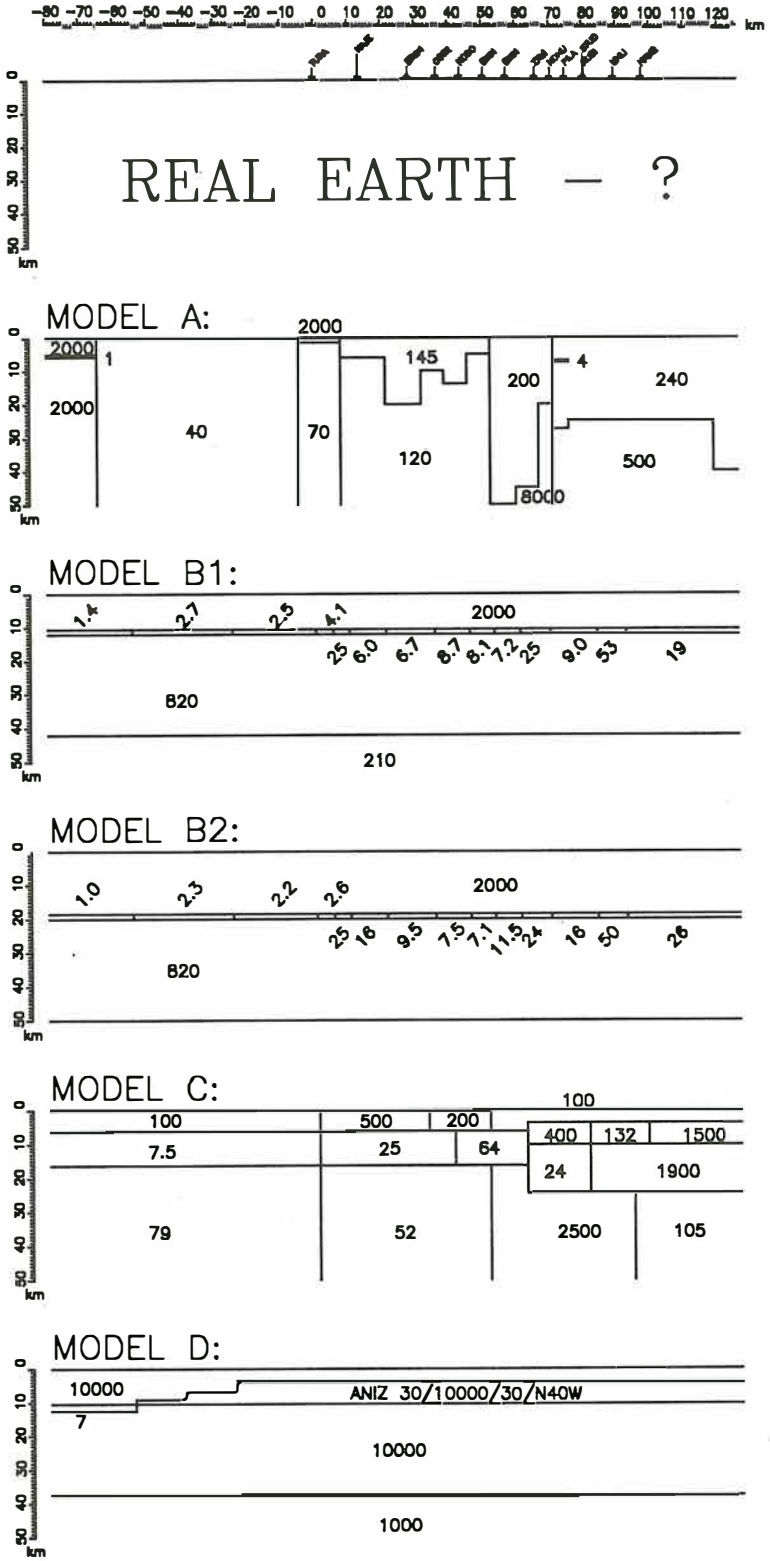

Figure 8: Models used to analyze MT data in SW Bohemia. The indices of blocks are for their resistivities in Ωm.

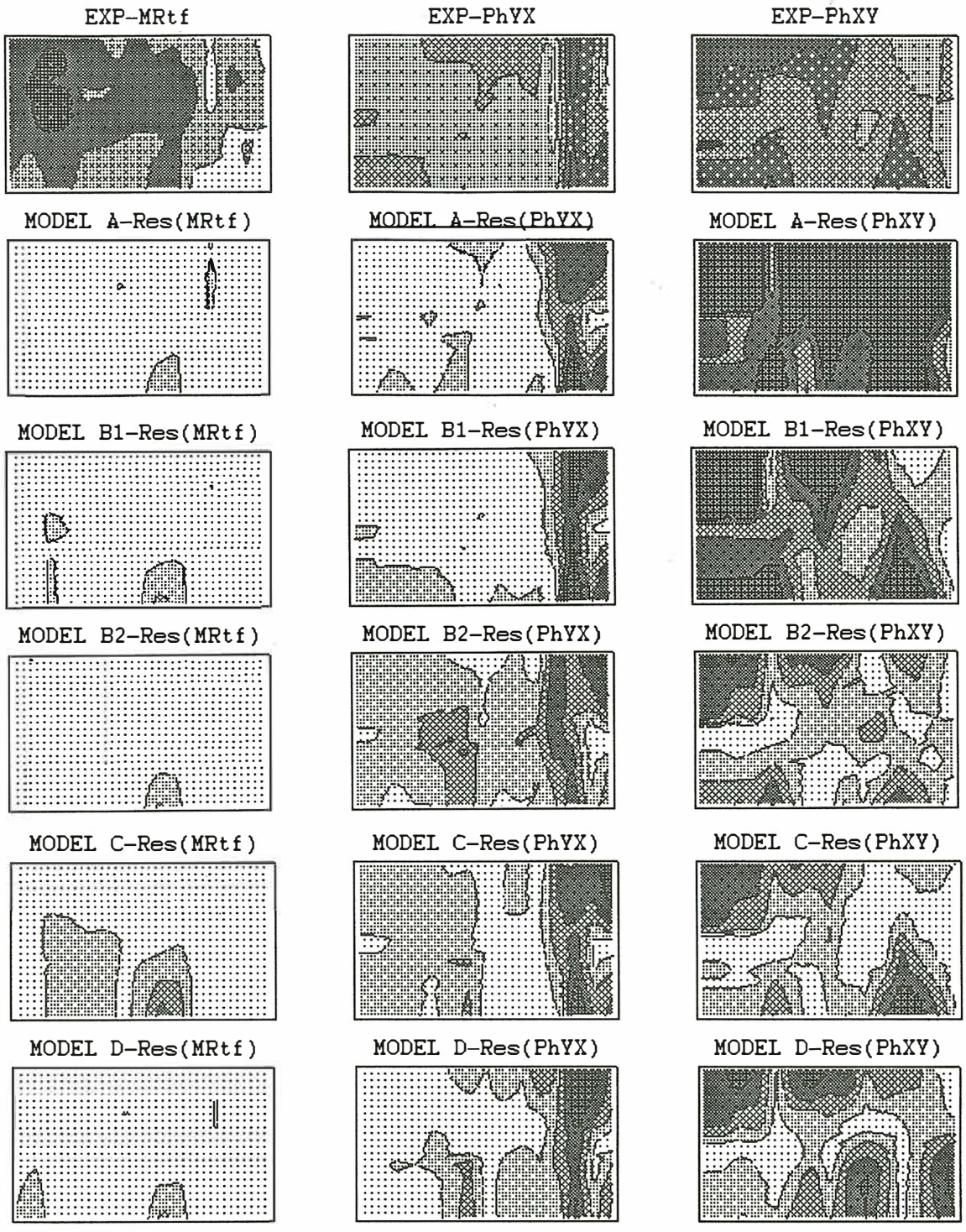

Figure 9: Gray scale plots of experimental moduli of the real induction arrows and impedance phases for Z_{yx} and Z_{xy} along the MT profile for periods from 10 to about 3000 s (top row). Below, gray scale plots of residuals of modelling results with respect to the experimental data are given for models from Fig. 8. Contours between the shaded zones, ordered, as a rule, from light to dark, are, for parametric plots, 0.05 to 0.30, step 0.05, for the moduli of induction vectors, and 20 to 70, step 10, for both phases. For residual plots, they are 0.05 to 0.20, step 0.05, for residuals of induction vectors, and 5 to 20, step 5, for phase residuals. Horizontal axes—distance along the profile from 0 to 100 km, vertical axes—logarithm of period from 10 to 3000 s.

various interpretation techniques. All models discussed below are summarized in Fig. 8. In Fig. 9 the gray scale plots of *residuals* of the modelling results with respect to the experimental data are shown for each of the models for the three MT/MV functions involved—module of the real induction vector, and phases of Z_{yx} and Z_{xy} impedances. Residuals seem to to illustrate the (mis)fit of the model data to experiment better than the parameter plots. In general, the darker the shading, the greater the residual in Fig. 9.

Initial approximation for MODEL A (Fig. 8) was a structure with a single well conducting block far beyond the northern end of the profile. The rest of the model was 'empty', i.e. a homogeneous layer was assumed, which was arbitrarily subdivided into several blocks. Marquardt's algorithm [11] was used to invert for resistivities of the blocks, and later, after electrical differentiation of blocks occured, also for the geometry of inter-block boundaries. Only moduli of real induction vectors were inverted in this experiment. As a result of the inversion, a block structure was generated without any particular features, with realistic resistivities. The fit to the experimental real induction vectors is practically perfect (Fig. 9). The phases, however, display unacceptably large differences as compared with the experimental data—the model phases are in general too low, indicating thus a need for a better conducting body below the profile.

In MODELs B such a conductor was inserted into the structure in a form of a conducting thin layer, as proposed by Eisel [5] and Tauber [6]. By segmenting the layer into zones of different resistivities, a gradual decrease of the electrical conductivity towards the S, as well as local fluctuations of MT/MV data can be modelled. To simulate the principal source of induction vectors, an extremely conducting segment was included into the layer at the northern margin of the model. As for MODEL A, Marquardt's algorithm was used again, now to invert moduli of real induction vectors and E-mode phases for resistivities of individual blocks. The inversion was repeated with the conducting thin layer placed at various depths, ranging from 10 to 25 km. The particular models B1 and B2 in Fig. 8 show inversion results for the conducting layer at the depths of 10.5 and 18.5 km. In all inversion runs, a very good fit of real induction vectors was achieved, illustrating again the poor resolution of MV data to vertical conductivity features within the structure. In comparison with MODEL A, phases improved substantially for both polarizations in MODELs B. With regard to H-polarization phases, MODEL B2, with the thin layer situated at greater depth, would be preferable.

Since our version of 2-D MT inversion [11], based on Marquardt's algorithm, is able to invert E-polarization data only, MODEL C was treated by a different inverse algorithm which is free of that restriction. The procedure was in principal a version of the controlled random search technique [10] extended to 2-D block models. The algorithm is rather demanding as far as computer resources are concerned. Nevertheless, a few experiments could be carried out with some success.

In MODEL C, all parameters, i.e. moduli of real induction vectors, as well as both E and H phases, were inverted for resistivities of the individual blocks. Though the fit to the experimental data is not so perfect as for MODELs B, mainly due to extremely slow convergence of the inversion procedure, the main features of the data are expressed in the results. Notice the dipping insulator below the southern section of the profile, which can also contribute to the anisotropy of MT phases.

The last model presented, MODEL D, tries to at least qualitatively cope with the apparent resistivities, which have been, as highly distorted, ignored in all previous modelling experiments. MODEL D, in an extremely speculative fashion, extrapolates Eisel's idea [12] on a highly anisotropic block, striking approximately NW-SE, emerging immediately below the KTB site, which can explain the observed AMT data in this area. Although this idea may be sound in the immediate vicinity of the KTB site, and may be physically substantiated as an effect of virtually observed steep dipping structures of high resistive rock interspersed with graphitized fracture zones, it is of rather speculative and unsubstantiated nature when extended to the regional scale. Nevertheless, as an experiment, MODEL D yields rather interesting results. First, it fits the induction vectors and phases almost equally well as the preceding models. Moreover, the extremely anisotropic crustal layer within the model (resistivities 30/10000/30 Ωm, anisotropy strike N40W degrees) excites highly anisotropic impedances along the profile, with anisotropy ratios typically close to 10. Minor axes of polar impedance diagrams are directed nearly exactly into the direction of preferred conductivity of the anisotropic layer, whereas the orientation of the induction arrows is practically unaffected. There is only a slight deflection, within 20 degrees at most, of the azimuths of real induction arrows, easternwards in the N and westernwards in the S of the profile. But similar azimuth variations are observed in experimental induction arrows as well (Fig. 2). For all these features, MODEL D, even though highly speculative, may be considered a successful equivalent model for the structure involved, at least.

8 Conclusion

We tried to present a few modelling results for long period MT and MV data from SW Bohemia which could help to decide on several structural features of the deep geoelectrical section below that geologically and tectonically quite intricate area. The principal conclusions can be summarized as follows:

(i) With regard to induction vectors, the deep, over-regional structure in the region exhibits a quasi–2-D character with structural strike in approximately the E-W direction.

(ii) Although seemingly inconsistent with the preceding item, MT data do not virtually contradict that conclusion, as they allow to be decomposed into a local and regional part. The regional MT strike seems to be approximately consistent with that indicated by induction arrows.

(iii) A well conducting layer at depths of 10 to 20 *km* is required within the 2-D regional structure throughout a substantial part of the profile, to explain MT phases properly.

(iv) The distorting near-surface layer, which can extend, owing to long periods used and generally high resistivities, as much as several kilometers beneath the earth's surface, exhibits considerable anisotropy with a strong regional part, striking NW-SE to NNW-SSE. Equivalent models with anisotropic blocks require huge anisotropies of 10^2–10^3, in terms of the anisotropy ratio, to be considered within the upper crust, to fit the experimental data.

Rather striking similarity between our MT/MV data and those obtained on the German side of the KTB environ (e.g. [4, 5, 6]), is in favour of the idea of structural continuity of the western margin of the Bohemian Massif throughout the region demarcated by the Franconian line in the W and the West Bohemian fault zone in the E, at least.

There are more features of the geoelectrical structure which we have not even touched on in this contribution. Particularly, the local anomalous distortions at station BRAN, as well as a pronounced anomaly near the southern end of the profile, when it passes into Šumava Moldanubicum, have not been discussed here. In both those areas additional AMT measurements have been carried out recently, and the results will be presented, after the interpretation is completed, elsewhere.

References

[1] Haak, V., Stoll, J. & Winter, H., 1991. Why is the electrical resistivity around the KTB hole so low?, *Phys. Earth Planet. Int.,* **66,** 12–33.

[2] Suk, M. et all., 1984. *Geological history of the territory of the Czech Socialistic Republic,* Ústř. ústav geol. Prague. Published by Geolog. Survey Prague, Academia, Prague, 17–33.

[3] Červ, V., Pek, J., Pěčová, J. & Praus, O., 1993. Electromagnetic measurements in the vicinity of the KTB drill site. Part I: The MV results across a 2-D array, *Studia Geophys. et Geodaet.,* **37,** 83–102.

[4] Bahr, K., 1990. Zur Zusammenlegung der Zerlegungen, in *Protokoll Kolloquium Elektromagnetische Tiefenforschung, Hornburg, 19–23 März 1990,* eds Haak, V. & Homilius, J., Niedersächsisches Landesamt für Bodenforschung, Hannover, 87–106.

[5] Eisel, M., 1990. Über die Superposition von lokalen and regionalen Leitfähigkeitsanomalien, untersucht anhand magnetotellurischer Messungen entlang eines Nord-Süd-Profils im Nordosten der Oberpfalz, *Diploma thesis,* Inst. für Meteor. und Gephys., Johann–Wolfgang–Goethe–Universität Frankfurt/M., 135 pp.

[6] Tauber, S., 1993. Die Leitfähigkeitsverteilung in den nördlichen Varisziden untersucht mit den Methoden der Magnetotellurik und der geomagnetischen Tiefensondierung auf einem Profil vom Oberpfälzer Wald ins Vogtland, *Diploma thesis,* Inst. für Geol., Geophys. und Geoinform., Freie Universität Berlin, 102 pp.

[7] Červ, V., Pek, J., Pěčová, J. & Praus, O., 1993. Electromagnetic measurements in the vicinity of the KTB drill site. Part II: Magnetotelluric results, *Studia Geophys. et Geodaet.,* **37,** 168–188.

[8] Bahr, K., 1991. Geological noise in magnetotelluric data: a classification of distortion types, *Phys. Earth Planet. Int.,* **66,** 24–38.

[9] Červ, V., Pek, J. & Praus O., 1993. MT and MV measurements in SW Bohemia. In *KTB-Report,* (submitted).

[10] Martinez, M., M., 1988. Grundlagen neuerer Inversionsmethoden und ihre Anwendung auf 1-D Inversion in der Magnetotellurik, in *Protokoll Kolloquium Elektromagnetische Tiefenforschung, Königstein im Taunus, 1–3 März 1988,* eds Haak, V. & Homilius, J., Niedersächsisches Landesamt für Bodenforschung, Hannover, 97–107.

[11] Pek, J., 1987. Numerical inversion of 2D MT data by models with variable geometry. *Phys. Earth Planet. Int.,* **45,** 193–203.

[12] Eisel, M., 1992. Effects of lateral anisotropic conductivity structures on magnetotelluric data, Contributed paper at the *11th Workshop on Electromagnetic Induction in the Earth, held on 26 August – 2 September 1992 at the Victoria University of Wellington,* Wellington, New Zealand.